Research Note : SHWS Inlet Water Temperature and Clear Sky Radiative Cooling

Prepared for Energy Efficiency Division, Department of Industry

Stage 1 - Climate zone map for solar hot water heaters - 13th June 2014 – edited 4th December 2015

Author: Dr Eric L Peterson, PhD, RPEQ, M-AIRAH, M-ASHRAE

With reference to "Heated water systems—Calculation of energy consumption" AS/NZS 4234:2008, and "NatHERS Reference Meterological Year climate files 2012" downloaded from the URL https://www.niwa.co.nz/node/109982, the present report forms "Stage 1 – Solar hot water demand and performance" of the contract "Climate zone map for solar hot water heaters" executed by the Commonwealth Department of Industry 22nd May 2014 for research by The University of Queensland in consortium with the National Institute of Water and Atmospheric Research, NIWA NZ.

The brief was to conduct a literature review to examine suitable models to estimate infrared radiative cooling under clear sky conditions on the basis of coincident dewpoint and cloud cover, and to determine the relationship between shallow earth temperature and inlet water temperature for solar hot water systems (SHWS).

In addition, a comparative study of solar hot water system performance is provided with respect to local meteorological conditions in terms of demand and solar resource at five key locations in Australia and New Zealand: Rockhampton (QLD), Richmond (NSW), Canberra (ACT), Auckland (NZ), and Dunedin (NZ). Trade literature and industry liaison were employed to nominate a typical flatplate rooftop installation suitable for these locations, with a pumped 250 litre storage tank.

It is relevant that the New Zealand House Energy Rating Scheme (NZHERS) files were developed by NIWA with the same approach as the NatHERS 2012 files, and so both sets of data are employed to compare performance at the five key locations. The present report employs the latest version of the University of Wisconsin's TRaNsient SYstems Simulation Studio TRNSYS 17 with a generic SHWS template.

In the present study explicit direct, diffuse, and global radiation as well as drybulb and dewpoint temperatures and windspeeds of the NatHERS and NZHERS TMY2 files are compared for the five key locations.

Contact: School of Civil Engineering

Level 5, Room 555, Advanced Engineering Building (49)

The University of Queensland

St Lucia QLD 4072

Relationship between shallow earth and inlet water temperature for solar hot water systems

With respect to the assessment of cold water inlet temperatures entering water heaters, the following literature review evaluates the appropriateness of utilizing the shallowest ground temperature (0.5 m) provided by the TMY2 files that have been developed by NIWA for NatHERS 2012 and EECA 2008. Before release of the NatHERS 2012 files this year, Australian Greenhouse Office 2006 files were used together with EECA 2008 files to produce the classification map in figure 1 below.

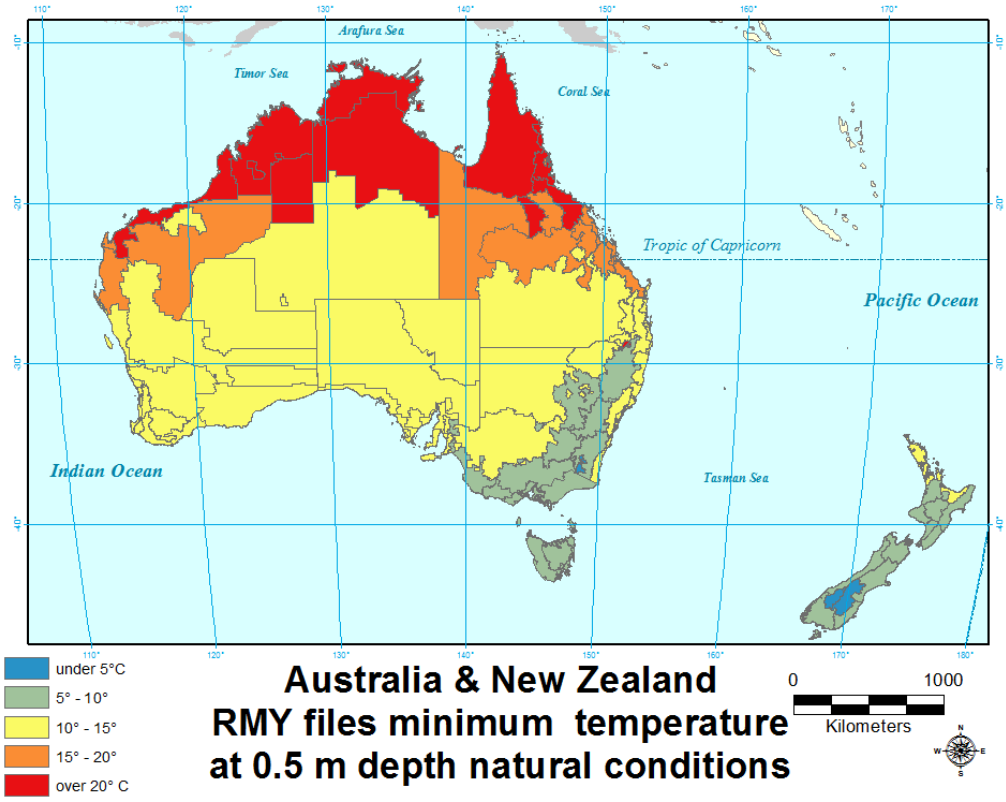

Figure 1 Minimum monthly shallow ground temperature (0.5 m) mapped with NIWA EECA 2008 TMY2 files and Australia Greenhouse Office 2006 RMY files obtained from the EnergyPlus Weather data.

Note EnergyPlus Weather Conversion Program (Crawley and Lawrie 2012) output states that the default soil diffusivity 2.322576× 10^{-3} m²/d which would equate to 2.7× 10^{-8} m²/s, and does not seem sensible. Therefor it is surmised they employ a default of 0.025 ft²/h = 2.322576 × 10^{-3} m²/d = 6.4516 × 10^{-7} m²/s soil diffusivity.

In special cases of steady-state conduction, thermal conductivity $\boldsymbol{k}$ may be the only soil property of interest. But underground temperature is driven by seasonal oscillations of summer and winter, and so the soil thermal diffusivity $\boldsymbol{\alpha}$ must be determined, being the ratio of thermal conductivity to the product of the soil density and specific heat $\boldsymbol{k/\rho \cdot C_p}$. EnergyPlus default k_{soil} = 1.0 W/m²·K; ρ=1200 kg/m³; and C_p = 1200 J/m³·K, and thus α = k/ ρ·C_p = 6.9 × 10^{-7} m²/s (7% more than 0.025 ft²/h).

Under slabs Krarti, et al. (2001) found α = 4.47 × 10^{-7} m²/s corresponds to soil thermal conductivity of k = 21 W/m·K which can be rearranged in terms of under-slab thermal mass, ρ·C_p = 47 MJ/m³·K.

Soil properties vary $\alpha_{sandy\ soil} = 0.24 \times 10^{-6}$ m²/s; $\alpha_{clay\ soil} = 0.18 \times 10^{-6}$ m²/s; $\alpha_{rock} = 1.43 \times 10^{-6}$ m²/s (Atkins 2007). Soil thermal conductivity in the range 0.6 to 3.5 W/m·K corresponds to thermal diffusivities in the range of 3×10^{-6} to 1.74×10^{-7} m²/s (Zhong and Braun 2007). Wikipedia gives diffusivity $\alpha_{water@25°C} = 0.143 \times 10^{-6}$ m²/s; $\alpha_{sandstone} \approx 1.14 \times 10^{-6}$ m²/s; α_{brick} 5.2×10^{-7} m²/s.

To understand the ground temperature data available from EnergyPlus TMY2 files recently released, it is worth viewing the Moorabbin (Melbourne suburb) data with "Climate Consultant" software in Figure 2 below, noting that the ground surface is assumed to be freshly mowed grass. Shallow 0.5m ground temperature varies 10 to 18°C, while AS/NZS 4234 zone 4 (Melbourne) varies 8 to 20°C. Monthly average air temperatures vary 9 to 19°C. Note that Yarra Valley Water network mean water mains varied 11 to 21°C, with extreme outliers in some branch lines 9 to 27°C (Bors and Kenway 2014).

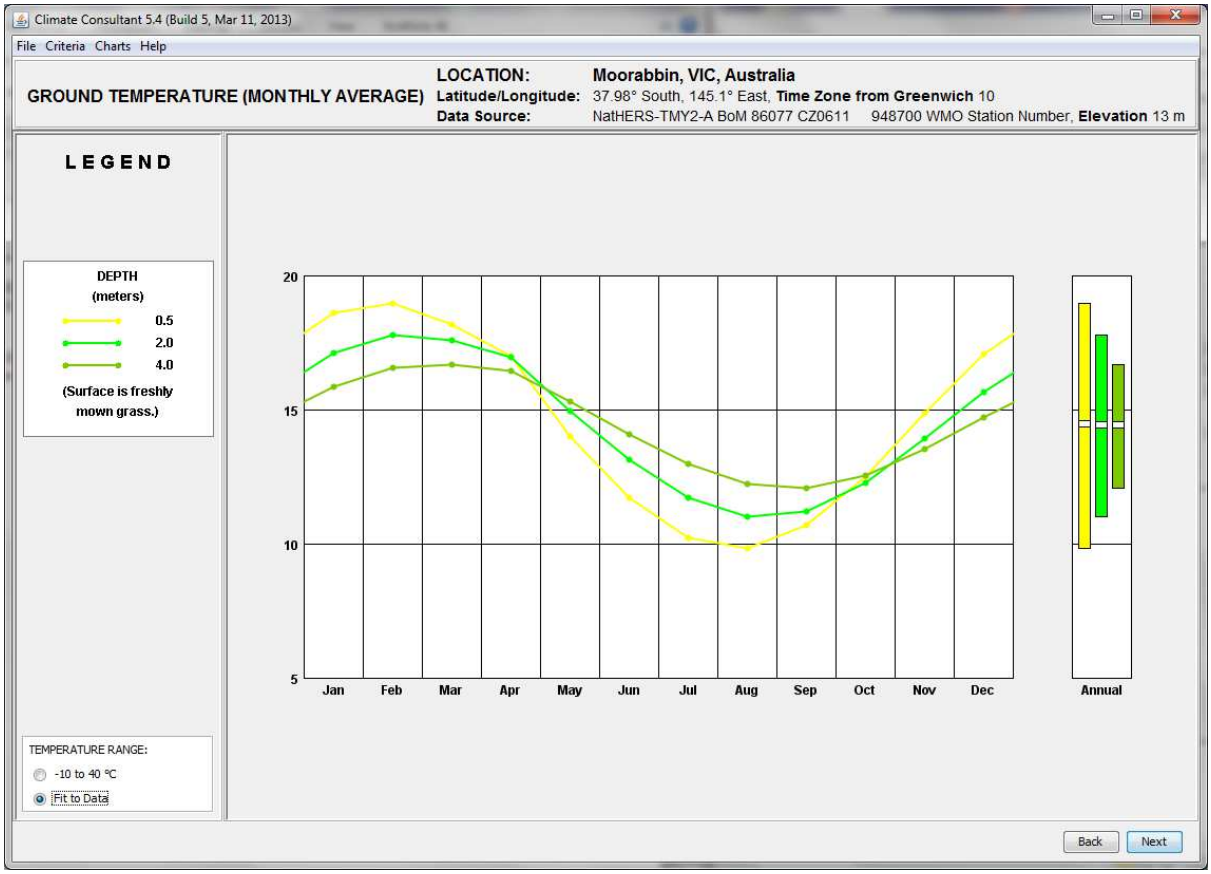

Figure 2 Moorabbin EnergyPlus TMY2 ground temperatures at 0.5m, 2m and 4m below surface, viewed with ClimateConsultant software version 5.4, available from the URL http://www.energy-design-tools.aud.ucla.edu/climate-consultant/request-climate-consultant.php after preprocessing with EnergyPlus Weather Statistics and Conversion version 7.2.6

The dissipation of fluid energy in water mains amounts to only a tiny fraction of one degree of temperature (Cabrera, et al. 2010), and so the most significant factors determining temperature of water mains are the ambient temperature as illustrated in Figure 3 from Burch and Christensen (2007).

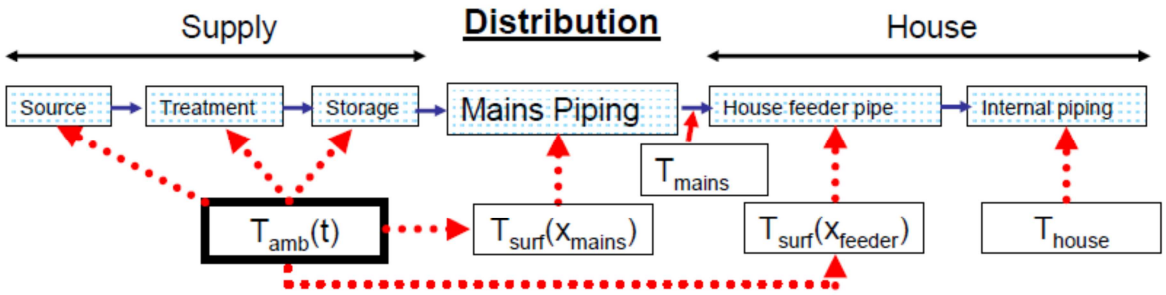

Figure 3 Burch and Christensen (2007) 's block diagram of a potable water supply system, showing importance of T_{amb} on T_{mains}. Copyright American Solar Energy Society, with rights retained by US Department of Energy, URL http://www.nrel.gov/docs/fy12osti/54539.pdf.

The influence of the temperature of the ground T_{grd} surrounding water mains at depth z_{pipe} is illustrated in Figure 4 from Burch and Christensen (2007), where surface temperature varies from ambient, which is elaborated upon by Popiel, et al. (2001) denoted by ΔT_m or ΔT_{offset}.

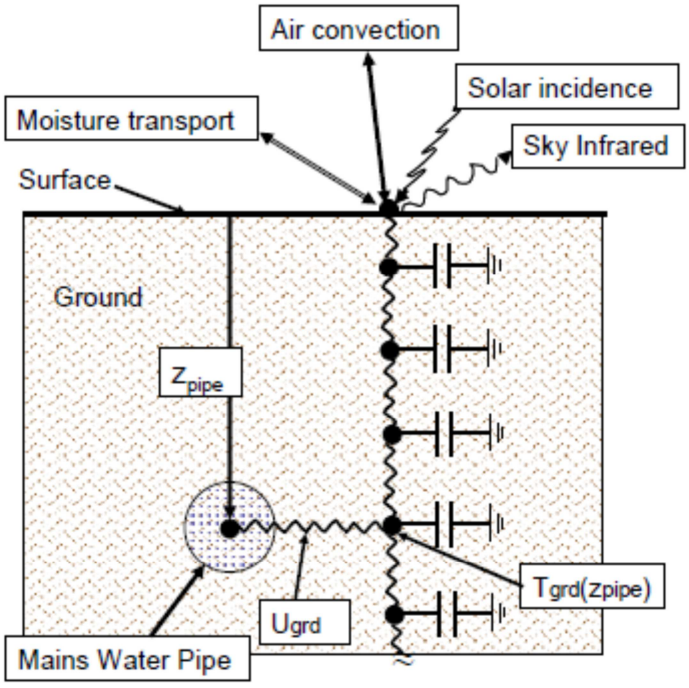

Figure 4 Burch and Christensen (2007)'s buried pipe schematic, with surface energy balance terms and schematic heat transfer model. Copyright American Solar Energy Society, with rights retained by US Department of Energy, URL http://www.nrel.gov/docs/fy12osti/54539.pdf

The Baggs equation is presented below in form suiting the southern hemisphere (Popiel, et al. 2001):

$$T(z,t) = (T_m + \Delta T_m) - 1.07\, K_v\, A_s \exp\{-0.00031552\, (z/\sqrt{\alpha})\} \cdot \cos[2\pi/365\, (t - t_o - 0.018335\, (z/\sqrt{\alpha}))]$$

where T_m = annual mean air temperature (°C)
ΔT_m = Bagg's correction to ground temperature at depth (K)
K_v = vegetation coefficient (K_v = 1 for bare ground; K_v = 0.22 for 100% cover)
A_s = amplitude of monthly average air temperature (K)
z = depth underground (m)
α = thermal diffusivity (m²/s)
t = timescale date (Julian date with year)
t_o = lag date corresponding to minimum air temperature

Burch and Christensen (2007) in Phoenix example used k=1 W/m·K and ρ=3000 kg/m³ and C_p= 1254 J/kg·K, so $\alpha = 2.66 \times 10^{-7}$ m²/s soil diffusivity. Burch and Thornton (2012) recommend the rating of water heaters with mains water temperature depending on air temperature

$$T_{mains} = T_{amb,avg} + \Delta T_{offset} + R\, \Delta T_{amb} \sin(\omega_{ann}\, t - \phi_{mains})$$

where R=0.05 and $\Delta T_{amb} = (T_{mon,max} - T_{mon,min})/2$ with $\phi_{mains} = a_3 + a_4\, T_{amb,ann}$ set to give minimum in late winter, $R = a_1 + a_2\, T_{amb,ann}$, and ΔT_{offset} = 2.8°C, and $\omega_{ann} = 2\pi/365$.

$a_1 = 0.4$;

$a_2 = 0.0056\ K^{-1}$;

$a_3 = 0.61$ radians; (I suggest adding π radians for southern hemisphere)

a_4 =-0.000314 radians per Kelvin

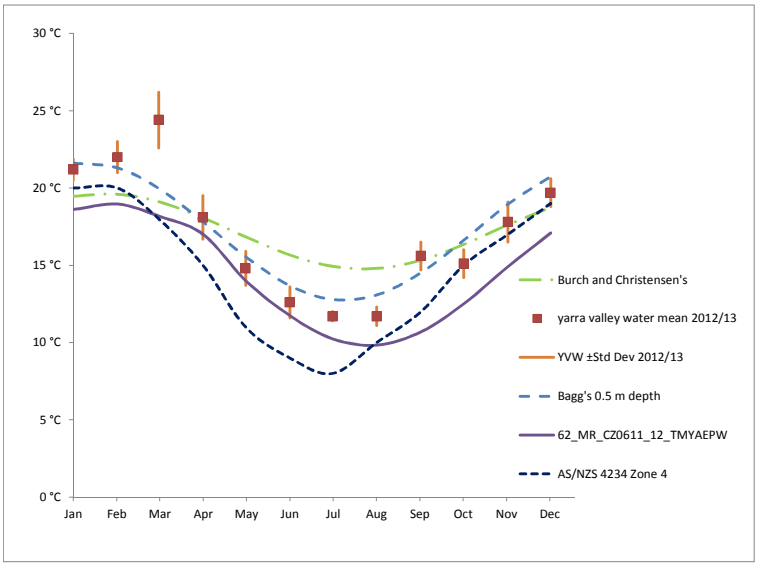

Figure 5 comparing Moorabbin TMY2 file 0.5 m deep ground temperature to AS/NZS 4234 zone 4 and Yarra Valley Water measurements April 2012 through March 2013. Baggs's formula for 0.5 m depth soil temperature with soil diffusivity $\alpha = 3 \times 10^{-3}$ m²/s and ΔToffset = 2.8 °C is good fit.

AS/NZS 4234:2008 cold water feeder temperatures for zone 4 (Melbourne) were proven to be several degrees too low in study of Yarra Valley Water (Bors and Kenway 2014). Figure 5 indicates that TMY2 0.5 m depth soil temperature is also conservative, but not as punitive as AS/NZS 4234. In figure 5 the heightened water mains temperatures observed in the Yarra Valley Water mains in March 2013 are not continuous with April 2012 commencement of the study by Bors and Kenway.

Figure 6 indicates when the TMY2 0.5 m depth ground temperatures are more conservative than AS/NZS 4234 cold water feeder temperatures at Rockhampton, Richmond, Moorabbin, Canberra, Auckland, and Dunedin. Except in the case of Canberra, the annual average is neutral or more conservative by accepting the TMY2 EnergyPlus 0.5 m depth ground temperature to represent cold water feeder temperatures. Canberra TMY2 EnergyPlus 0.5 m depth ground temperature average is 1 °C higher than AS/NZS 4234 cold water feeder temperatures, averaged over the year. Perhaps a water mains network study should be commissioned, but the results from Yarra Valley Water show that either AS/NZS 4234 or TMY2 EnergyPlus 0.5 m depth ground temperature provide a lower estimate of water mains temperature in the vicinity of Moorabbin, and so it seems reasonable to accept the NatHERS 2012 and EECA 2008 EnergyPlus TMY2 files 0.5 m depth ground temperature as a conservative surrogate for water mains temperature in the 87 house energy rating zones of Australia and New Zealand.

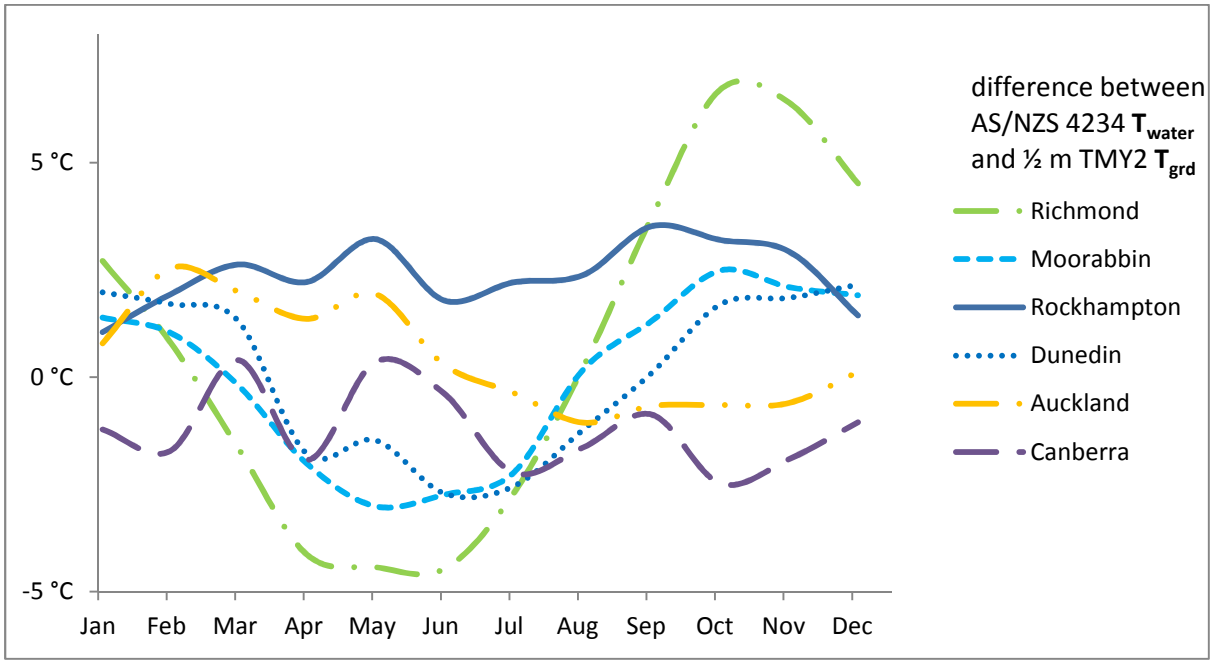

Figure 6 Comparing AS/NZS 4234 T_{water} and T_{grd} derived from TMY2 EnergyPlus Weather ½ m depth. Note positive values indicate that AS/NZS 4234 T_{water} > $T_{grd(½m)}$, as conservative assumption.

Rockhampton TMY2 0.5m depth varies 18 to 27°C; AS/NZS 4234 cold water ranges 20 to 28°C.

Richmond TMY2 0.5m depth varies 12 to 23°C; AS/NZS 4234 (Sydney) cold water varies 11 to 23°C.

Canberra TMY2 0.5m depth varies 7 to 20°C; AS/NZS 4234 cold water varies 5 to 19°C.

Auckland TMY2 0.5m depth varies 12 to 19°C; AS/NZS 4234 cold water ranges 11 to 21°C.

Dunedin TMY2 0.5m depth varies 7 to 14°C; AS/NZS 4234 cold water ranges 5 to 16°C.

Infrared radiative cooling relationship to dewpoint and cloud cover

With regard to modelling infrared radiative cooling, particularly under clear sky conditions, a review of models based upon dewpoint and cloud cover is provided herein. Because infrared sky radiation is not generally measured by standard meteorological stations, it must be estimated from other observations.

The phenomena of thermal radiation emission to the sky is modelled as hourly horizontal infrared (HIR) radiation in the 87 TMY2 files that have been developed by NIWA for NatHERS 2012 and EECA 2008. The default condition, as specified by EnergyPlus Weather Converter is that Opaque Sky Cover is taken at a constant 50% if cloud cover is not provided.

$$HIR = \epsilon_{sky} \times \sigma \times T_{db}^{4}$$

$$T_{sky} = (HIR/\sigma)^{1/4} - 273.15$$

where

HIR is the horizontal IR intensity {W/m2}

T_{sky} is the radiative temperature of the sky if it were assumed to be a black body

ϵ_{sky} is the emissivity of the sky

σ is Stefan-Boltzmann constant {5.6697×10^{-8} W/m²·K⁴}

T_{db} is the absolute drybulb temperature {K}

According to Walton (1983) emissivity of the sky is calculated as follows

$$\epsilon_{sky} = (0.787 + 0.764 \times \log(T_{dp}/273)) \times F_{cloud}$$

where

T_{dp} is the absolute dewpoint temperature {K}

cloud cover factor, $F_{cloud} = (1 + 0.0224\ N - 0.0035\ N^2 + 0.00028\ N^3)$

N is the opaque sky cover {tenths}

For clear sky (N=0) with temperature T_{db} = 20°C+273 = 293K and dewpoint T_{dp} = 10°C+273 = 283K

In this example the emissivity of the sky, $\epsilon_{sky} = 0.787 + 0.764 \times 0.031 = 0.811$

Horizontal sky cooling, $HIR = 0.811 \times 5.6697 \times 10^{-8} \times (293^4) = 339$ W/m²

Other models of emissivity of clear sky are also related to dew point temperature.

$\epsilon_{sky} = 0.787 + 0.0028\ T_{dp}$ where T_{dp} is the dewpoint temperature expressed as °C

is known as the "trinity equation" (Clark and Allen 1978) while Chen et al. (1991) proposed the following variation, still with linear proportionality to dewpoint:

$\epsilon_{sky} = 0.787 + 0.006349\ T_{dp}$ where T_{dp} is the dewpoint temperature expressed as °C

Martin and Berdahl (1984) utilize and intermediate temperature $T_1 = 0.01\ (Tdp-273)$

$$\epsilon_{sky} = 0.711 + 0.01\ T_1 \times (0.56 + 0.73\ T_1)$$

Brown (1997) used parameters A_1= -0.0103; A_2= -6.1 x10-4; and $A_3 = 6.1 \times 10^{-6}$ P_v {kPa}

$$\epsilon_{sky} = 0.65 + 0.41\ P_v^{0.9} \times \exp\{\sum_{i=1}^{3} A_i(Ta - 240)^i\}$$

which uses P_v vapour pressure {kPa} instead of dewpoint as the independent variable.

The alternative models of clear sky emissivity are compared in figure 7, taken from Clear et al. (2001), where analysis was limited by lack of sky long-wave radiation measurements. They employed Walton's model, but did not justify why they believed it to be the most appropriate, but it seems likely that extraction of vapour pressure for Brown's equation was not an attractive task when there appears to be little difference from the simplistic Martin and Berdahl model based on dewpoint temperature.

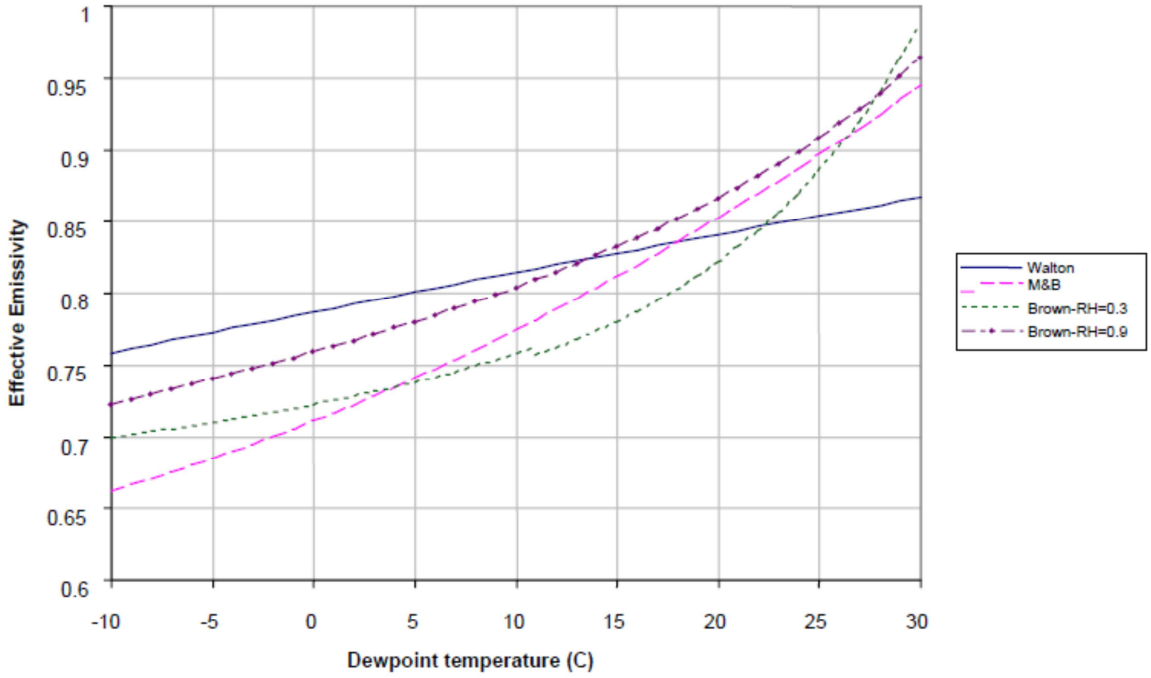

Figure 7 from Clear et al. (2001) Clear sky emissivity vs. dewpoint temperature as predicted by the Walton, Martin and Berdahl, and Brown models. Two values of relative humidity are shown for the Brown model. This figure was funded by US Department of Energy, Lawrence Berkeley National Laboratory.

Angstrom (1918) developed three-term empirical relationship between clear-sky emissivity and vapour pressure $\epsilon_{sky} = x_1 + x_2 \times 10^{-x3 \cdot P_v}$ which was simplified in two terms by Brunt (1932)

$$\epsilon_{sky} = x_1 + x_2 \times \sqrt{P_v}$$

where $x_1 = 0.55 \pm 13\%$ while $x_2 = 0.65\ hPa^{-0.5} \pm 32\%$ (Iziomon, et al. 2003)

Wang and Ling (2009) recommended $x_1 = 0.605$ and $x_2 = 0.048\ hPa^{-0.5}$

Duffie and Beckman (1991) reviewed sky temperature literature and commented that it is fortunate that variations between alternative models do not have a substantial impact on the performance of solar collectors. However they caution that sky temperature is critical in radiative cooling. Nearly horizontal

solar collectors can function as effective radiators to chill water in situations where night sky temperatures are substantially below ambient air, but dust build-up will degrade performance. An interesting correlation with ambient temperature T_{db} {K}, dewpoint T_{dp} {°C} and hour from midnight (Berdahl and Martin 1984) models sky temperature {K}.

$$T_{sky} = T_{db} \{0.711 + 0.0056\, T_{dp} + 0.000073\, T_{dp}^2 + 0.013 \cos(15\, t)\}^{0.25}$$

Cloudy sky HIR depends on either clearness index, cloud cover, or solar index – with various methods yielding an accuracy of about 10% in Swedish case studies (Wallentén 2010), recommending Dilley and O'Brian clear sky radiation with Kimball, et al. cloud adjustments.

Dilley and O'Brian (1998) use mm precipitable water $\boldsymbol{w} = 4650 \left(P_v / T_o\right)$ to predict clear sky radiation

$$HIR_{clear} = 59.38 + 113.7\, (T_o/273.16)^6 + 19.39 \sqrt{w}$$

Vapour pressure P_v is related to dewpoint by Tetens' equation (Murray 1967)

$$P_v = 0.61078 \times \exp[17.2694 \times (T_{dp} - 273.16)/(T_{dp} - 35.86)]$$

Kimball, et al. (1982) uses atmospheric transmittance in the 8-14 μm band, $\tau_8 = 1 - \epsilon_8$, and the fraction f_8 of black body radiation emitted in this band based on cloud temperature T_{cloud}

$$T_{cloud} = T_{db} - 0.0065\, Z_{cloud} \qquad (\text{nominal } T_{cloud} = T_{db} - 11°C)$$

$$f_8 = -0.6732 + 0.6240 \times 10^{-2}\, T_{cloud} - 0.9140 \times 10^{-5}\, T_{cloud}^2$$

$$\text{zenith emissivity } \epsilon_{8z} = 0.24 + 2.98 \times 10^{-6} \times P_v^2 \times P_v^{(3000/T_o)}$$

$$\tau_8 = 1 - \epsilon_{8z}\, (1.4 - 0.4\, \epsilon_{8z})$$

$$HIR_{cloudy} = HIR_{clear} + \tau_8\, C\, f_8\, \sigma\, T_{cloud}^4$$

where cloud fraction C = N/10

Wang and Liang (2009) found that daily HIR has been increasing at a rate of 2.2 W/m^2 per decade around the world due increases in air temperature, water vapour and CO_2 concentration.

Cloud Cover Remote Sensing

Satellite monitoring of cloud cover is well established (Ackerman, et al. 1998)

The Australian Bureau of Meteorology advises that the following channels are available for hourly analysis, and so discussions are on-going to establish if the NatHERS 2012 files could be improved to include night time cloud cover. Five bands are available within infrared coverage over Australia, provided by the Japanese Meteorological Satellites that have informed the solar data that is now included in the NatHERS 2012 TMY2 files.

Band: 1	0.73 μm VIS Cloud and Surface Features	1km
Band: 2	10.8 μm IR Surface/Cloud-top Temp	4km
Band: 3	12.0 μm IR SFC/Cloud Temp, Low-level WV	4km
Band: 4	6.75 μm IR Mid-level Water Vapour	4km
Band: 5	3.75 μm IR Low Cloud/Fog,Fire Detection	4km

The first band is of no use at night, so the 4km resolution bands 2 and 5 would suffice for cloud detection. The difference between the brightness temperatures measured in the shortwave (3.75 μm) and in the longwave (10.8 μm) window regions can be used to determine if cloud is present.

Grey Literature Review

In addition, a comparative study of solar hot water system performance is provided with respect to local meteorological conditions in terms of demand and solar resource at five key locations in Australia and New Zealand. Trade literature and industry liaison were employed to nominate a typical flatplate rooftop installation suitable for these locations: Rockhampton (QLD); Richmond (NSW); Canberra (ACT); Auckland (North Island, NZ); Dunedin (South Island, NZ). Note that the three Australian locations have been proposed by AS/NZS DR 102470, 102471, and 102472 (ISO 16358-1, 2, and 3: 2013) as representative of broadly defined residential heating and cooling demand zones ("Hot/Humid", "Mixed", and "Cold/Icing") based upon NatHERS Climate Zones 7, 28, and 24.

Although represented by Richmond (NSW) under the residential heating cooling scheme, Auckland has been separately analysed in the present report as it is the dominant population centre of New Zealand and also represents characteristics of the frost-free "winterless north" of the North Island. Although represented by Canberra (ACT) under the residential heating cooling scheme, Dunedin is the largest population centre beyond 45° latitude and exemplifies limited solar radiation and icing problems.

It is relevant that the New Zealand House Energy Rating Scheme (NZHERS) files were developed by NIWA with the same approach as the NatHERS 2012 files, and so are comparable.

Preliminary simulation with Transys 17

4.1 m² total collector area, installed on 25° north facing roof with 250 litre storage tank.

Assumed constant 38 MJ daily demand for 65°C hot water, heating from constant average temperature based on 0.5 m ground temperature from TMY2 files.

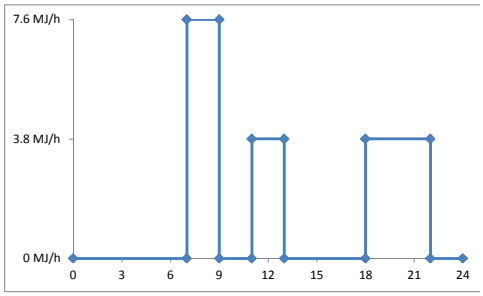

TABLE 1 Defining 38 MJ daily demand

location	inlet	demand
Rockhampton	22.5 °C	214 L/d
Richmond	17.0 °C	189 L/d
Canberra	13.3 °C	176 L/d
Auckland	15.4 °C	183 L/d
Dunedin	10.8 °C	168 L/d

Figure 8 Hourly load profile employed

Results of TRNSYS 17 simulations of the generic system are summarized in Table 2, with detailed hourly plots in Figure 9a, 9b, 9c, 9d, and 9e. Reading the right-most column "Fsol" it is found that Rockhampton requires only 1% auxiliary boost, while Dunedin would require boost to supply 32% of hot water energy per annum. The seasonal efficiency of collectors ranges 28 to 32% EtaColl, with the better performance in Dunedin due to the angle of installation. Note that IColl is the incident solar energy on the tilted collector surface, while QuColl is the energy harvested and used by solar hot water system.

Table 2 Summary results of preliminary simulations

location	TIME	IColl	QuColl	QDHW	QAux	EtaColl	FSol
Rockhampton	8760	8 kWh	11 MJ	7 MJ	0.1 MJ	28%	0.99
Richmond	8760	7 kWh	10 MJ	8 MJ	0.7 MJ	30%	0.91
Canberra	8760	7 kWh	11 MJ	9 MJ	0.8 MJ	29%	0.91
Auckland	8760	6 kWh	9 MJ	8 MJ	1.5 MJ	30%	0.82
Dunedin	8760	5 kWh	8 MJ	9 MJ	2.8 MJ	32%	0.68

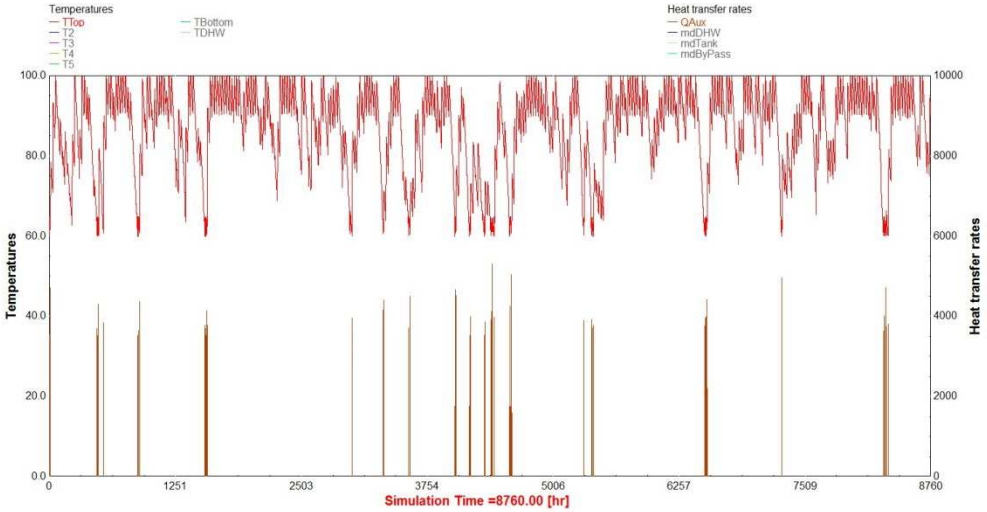

Figure 9a Rockhampton hourly results of storage temperature and booster demand

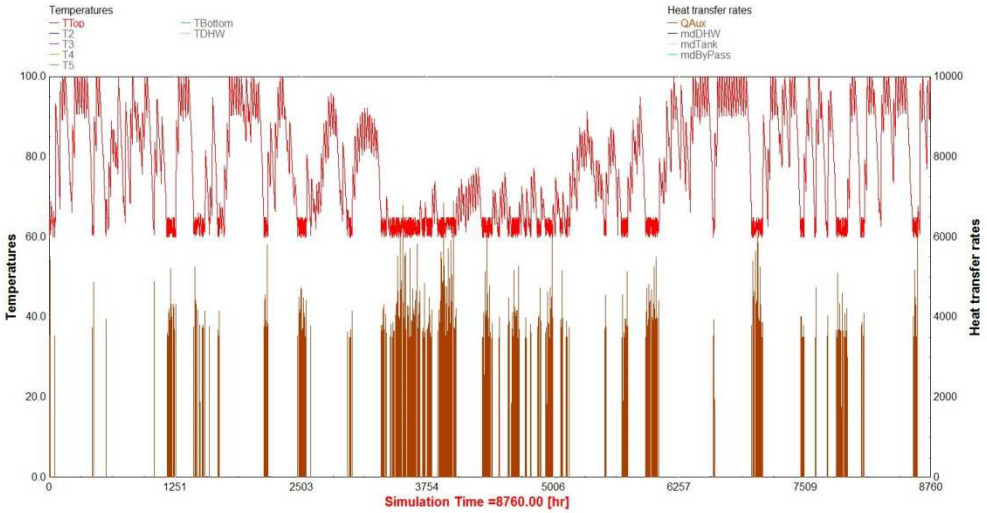

Figure 9b Richmond hourly results of storage temperature and booster demand

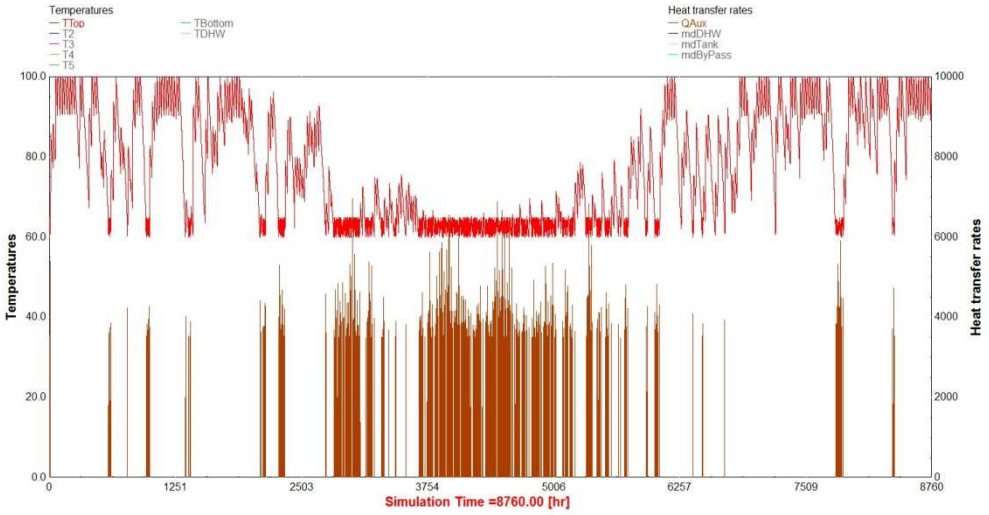

Figure 9c Canberra hourly results of storage temperature and booster demand

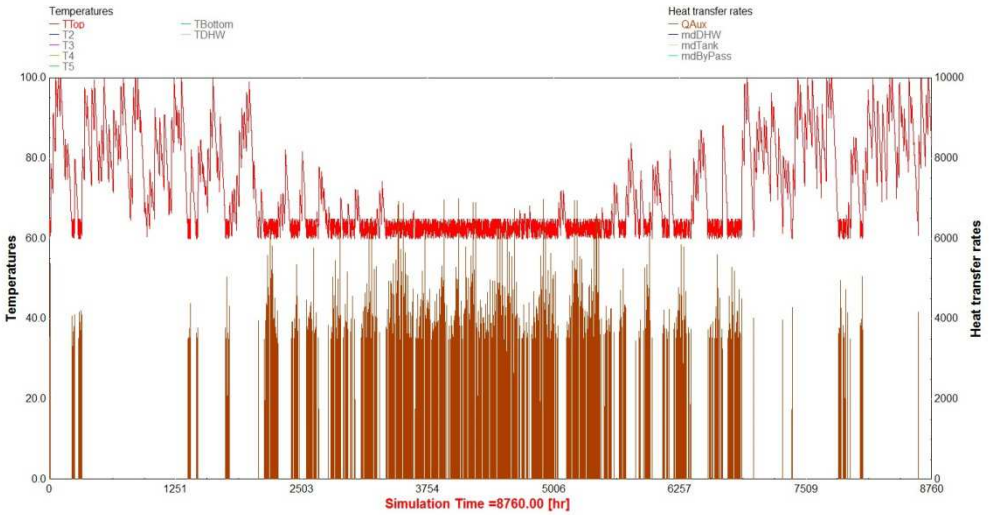

Figure 9d Auckland hourly results of storage temperature and booster demand

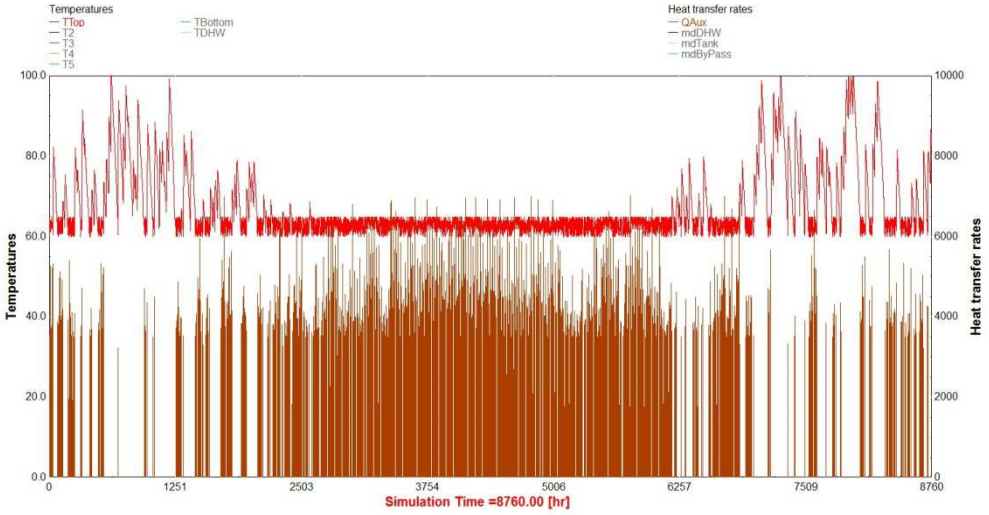

Figure 9e Dunedin hourly results of storage temperature and booster demand

References

Ackerman, S. A., Strabala, K. I., Menzel, W. P., Frey, R. A., Moeller, C. C., & Gumley, L. E. (1998). Discriminating clear sky from clouds with MODIS. Journal of Geophysical Research: Atmospheres (1984–2012), 103(D24), 32141-32157.

Ångström, Anders (1916). A study of the radiation of the atmosphere. Smithsonian Miscellaneous Collection, 65: 1–159

Brown, D (1997). An improved meteorology for characterizing atmospheric boundary layer turbulence dispersion. Ph.D. Thesis, Department of Mechanical and Industrial Engineering, University of Illinois at Urbana-Champaign.

Brunt, D (1932). Notes on radiation in the atmosphere, Q. J. Roy. Meteorol. Soc., 58:389–420

Walton, G. N. 1983. Thermal Analysis Research Program Reference Manual. NBSSIR 83-2655. National Bureau of Standards, p. 21.

Clark, G. and C. Allen, "The Estimation of Atmospheric Radiation for Clear and Cloudy Skies," Proceedings 2nd National Passive Solar Conference (AS/ISES), 1978, pp. 675-678.

Clear, R. D., Gartland, L., & Winkelmann, F. C. (2001). An Empirical Correlation for the Outside Convective Air Film Coefficient for Horizontal Roofs. http://gundog.lbl.gov/dirpubs/47275.pdf

Chen, B., Kasher, J., Maloney, J., Girgis, A., & Clark, D. (1991). Determination of the clear sky emissivity for use in cool storage roof and roof pond applications. In Proc. ASES Annual Meeting. http://www.ceen.unomaha.edu/solar/documents/SOL_26.pdf

Duffie, JA and Beckman, WA (1991). Solar Engineering of Thermal Processes (2nd Ed). Wiley Interscience, New York.

Wallentén, P. (2010). The Treatment of Long-Wave Radiation and Precipitation in Climate Files for Building Physics Simulations.
http://web.ornl.gov/sci/buildings/2012/2010%20B11%20papers/111_Wallenten.pdf

Iziomon, MG, Mayer, H, & Matzarakis, A (2003). Downward atmospheric longwave irradiance under clear and cloudy skies: Measurement and parameterization. Journal of Atmospheric and Solar-Terrestrial Physics, 65(10), 1107-1116.

Kimball, B.A., S.B. Idso, and J.K. Aase. 1982, A model of thermal radiation from partly cloudy and overcast skies. Water Resources Research 18:931–36.
http://naldc.nal.usda.gov/naldc/download.xhtml?id=54883&content=PDF

Liu Jian, Xu Jianmin (2008). An automated, dynamic threshold cloud detection algorithm for FY-2C images. Eighth International Winds Workshop, NMSC, Beijing, China, April 2006.

Walton, G.N. (1985). Thermal Analysis Research Program- Reference Manual, NBSIR 83-2655, U.S. Department of Commerce, March 1983, Update 1985.

Wang, K., & Liang, S. (2009). Global atmospheric downward longwave radiation over land surface under all-sky conditions from 1973 to 2008. Journal of Geophysical Research: Atmospheres (1984–2012), 114(D19).

Martin M, and Berdahl P (1984). Characteristics of infrared sky radiation in the United States. Solar Energy 33:321-336.

Nordeen, M. L., Doelling, D. R., Minnis, P., Khaier, M. M., Rapp, A. D., & Nguyen, L. (2001, March). GMS-5 satellite-derived cloud properties over the tropical western Pacific. In Proceedings of 11th ARM

Murray, F. W. (1967). On the computation of saturation vapor pressure. Journal of Applied Meteorology, 6(1), 203-204.

Atkins, N. (2007). Basics of a soil layer model. Boundary Layer Meteorology, Lyndon State College http://apollo.lsc.vsc.edu/classes/met455/notes/section6/2.html

Bors, J, and Kenway, S. (2014). Water temperature in Melbourne and Implications for household energy use. Water-energy-carbon links in households and cities, The University of Queensland, 17 March 2014.

Burch, J., and Christensen, C. (2007). Towards development of an algorithm for mains water temperature. In PROCEEDINGS OF THE SOLAR CONFERENCE (Vol. 1, p. 173). AMERICAN SOLAR ENERGY SOCIETY; AMERICAN INSTITUTE OF ARCHITECTS.

Burch, J and Thornton, J (2012). A Realistic Hot Water Draw Specification for Rating Solar Water Heaters. World Renewable Energy Forum, Denver May 13-17, 2012.

Cabrera, E., Pardo, M. A., Cobacho, R., & Cabrera Jr, E. (2010). Energy audit of water networks. Journal of Water Resources Planning and Management, 136(6), 669-677.

Crawley, Drury B and Lawrie, Linda K (2012). EnergyPlus Weather Converter version 7.2.6. Bentley Systems and DHL Consulting LLC under contract to US Department of Energy.

Crawley, Drury B, Jon W H and, Linda K Lawrie. 1999. "Improving the Weather Information Available to Simulation ProgramsPDF," in Proceedings of Building Simulation '99, Volume II, pp. 529-536, Kyoto, Japan, September 1999. IBPSA.

Krarti, M, Chuangchid, P, and Ihm, P (2001). Foundation heat transfer module for EnergyPlus program. Seventh International IBPSA Conference, Rio de Janeiro, August 13-15, 2001.

Lockington, D. (2012). CIVL 4180 Sustainable Built Environment Lecture, "Baggs Formula of Ground Temperature Seasonal Variation". University of Queensland, School of Civil Engineering.

Popiel, C. O., Wojtkowiak, J., & Biernacka, B. (2001). Measurements of temperature distribution in ground. Experimental thermal and fluid science, 25(5), 301-309.

EnergyPlus (2013). Auxiliary EnergyPlus Programs. Extra programs for EnergyPlus. Lawrence Berkeley National Laboratory November 22, 2013. URL http://apps1.eere.energy.gov/buildings/energyplus/pdfs/auxiliaryprograms.pdf